Journal of Neurochemistry

JOURNAL OF NEUROCHEMISTRY | 2013 | 126 | 203–212 doi: 10.1111/jnc.12243

REVIEW

STED microscopy of living cells – new frontiers in membrane and neurobiology

Christian Eggeling,*,† Katrin I. Willig* and Francisco J. Barrantes‡

*Department of Nanobiophotonics, Max Planck Institute for Biophysical Chemistry, Göttingen, Germany

†Weatherall Institute of Molecular Medicine, University of Oxford, Oxford, UK

‡Laboratory of Molecular Neurobiology, Institute of Biomedical Research (BIOMED) UCA–CONICET, Catholic University of Argentina, Buenos Aires, Argentina

Abstract

Recent developments in fluorescence far-field microscopy such as STED microscopy have accomplished observation of the living cell with a spatial resolution far below the diffraction limit. Here, we briefly review the current approaches to super-resolution optical microscopy and present the implementation of STED microscopy for novel insights into live cell mechanisms, with a focus on neurobiology and plasma membrane dynamics.

Keywords: fluorescence imaging, membrane dynamics, STED nanoscopy.

J. Neurochem. (2013) **126**, 203–212.

Microscopy has revolutionized our understanding of life and matter, since it allows the observation of molecular organization in complex biological systems. Among all the different microscopy techniques, optical microscopy is one of the least invasive approaches: the use of light hardly influences the system under study. Optical microscopy of the living cell is usually applied in the far-field, where the use of a lens-based system and focused light allows the observation micrometers to millimeters away from the given optical element(s), preserving the non-invasiveness and the ability to observe deep inside living cells or tissues. Further, when combined with the fluorescence readout (e.g., fluorescent-labeled molecules), far-field fluorescence microscopy achieves the specific and highly sensitive detection of cellular constituents and thus permits the disclosure of molecular distributions and dynamics in the living cell.

However, a number of challenging issues in biology lie beyond the reach of conventional far-field optical microscopy, especially because of its limited spatial resolution. When using visible and focused light, light diffraction prevents the discernment of alike objects closer together than approximately 200 nm (Abbe 1873). A remedy to this physical limit is the reversible inhibition of fluorescence, ensuring that the measured signal stems from a region of the sample that is much smaller than 200 nm (Hell 2007). Starting in 1994 (Hell and Wichmann 1994) different far-field fluorescence super-resolution microscopy or nanoscopy approaches have emerged, all capable of achieving cellular imaging with – in principle – unlimited spatial resolution. Examples include optical Stimulated Emission Depletion (STED) (Hell and Wichmann 1994; Klar *et al.* 2000), Reversible Saturable Optical (Fluorescence) Transitions (RESOLFT) (Hell *et al.* 2003; Hofmann *et al.* 2005; Grotjohann *et al.* 2011) Ground State Depletion (GSD) (Hell and Kroug 1995; Bretschneider *et al.* 2007; Han *et al.* 2010) nanoscopy, Stochastic Optical Reconstruction Microscopy (STORM) (Rust *et al.* 2006), and (fluorescence)

Received December 14, 2012; revised manuscript received February 18, 2013; accepted March 13, 2013.

Address correspondence and reprint requests to Christian Eggeling, Department of Nanobiophotonics, Max Planck Institute for Biophysical Chemistry, Am Fassberg 11, 37077 Göttingen, Germany.
E-mail: ceggeli@gwdg.de

Abbreviations used: cLTP, chemical long-term potentiation; dSTORM, direct STORM; FCS, fluorescence correlation spectroscopy; GFP, green fluorescent protein; GSD, ground state depletion; GSDIM, ground state depletion microscopy followed by individual molecule return; LTD, long-term depression; LTP, long-term potentiation; PALM, photoactivated localization microscopy; PSF, point-spread-function; RESOLFT, reversible saturable optical (fluorescence) transitions; rsGFP, reversible switchable GFP; SIM, structured-illumination microscopy; SMACM, single-molecule active control microscopy; SPT, single-molecule or -particle tracking; STED, stimulated emission depletion; STORM, stochastic optical reconstruction microscopy; YFP, yellow fluorescent protein.

Photoactivated Localization Microscopy ((f)PALM) (Betzig *et al.* 2006; Hess *et al.* 2006). Detailed reviews of the different nanoscopy approaches, especially of their different technical aspects, can be found elsewhere (Hell 2003, 2007, 2009a, b; Hell *et al.* 2004; Moerner 2006; Heintzmann and Ficz 2007; Rice 2007; Bates *et al.* 2008; Dedecker *et al.* 2008; Fernandez-Suarez and Ting 2008; Chi 2009; Evanko 2009; Heilemann *et al.* 2009; Heintzmann and Gustafsson 2009; Huang *et al.* 2009, 2010; Lippincott-Schwartz and Manley 2009; Huang 2010; Patterson *et al.* 2010; Dempsey *et al.* 2011; Muller *et al.* 2012). After a brief overview of these approaches, we will restrict ourselves to the basic principles underlying recent developments in optical nanoscopy which make it a highly versatile tool for the observation of the living cell, taking STED nanoscopy as an example and focusing on neurobiology and plasma membrane dynamics.

The principle of fluorescence nanoscopy

Differing in their technical details, all of the aforementioned fluorescence nanoscopy approaches are based on the principle of reversibly inhibiting the fluorescence emission of the cellular labels (Hell *et al.* 2003; Hell 2004, 2007) (Fig. 1).

STED (Hell and Wichmann 1994; Klar *et al.* 2000), GSD (Hell and Kroug 1995; Bretschneider *et al.* 2007; Han *et al.* 2010) or more generally RESOLFT (Hell *et al.* 2003; Hofmann *et al.* 2005; Grotjohann *et al.* 2011) nanoscopes use a targeted or deterministic approach by inhibiting the fluorescence at pre-defined spatial positions, as outlined in the examples in Fig. 1a: a laser beam that excites fluorescence, that is, which switches fluorescence ON, is focused onto a small (diffraction-limited) spot. Scanning this spot over the sample and detecting the fluorescence for each scanning position permits the reconstruction of an image by providing the spatial distribution of the fluorescent-labeled molecules (as is for example realized in a confocal microscope). The spatial resolution is given by the so-called point-spread-function (PSF) of the microscope, which for the scanning microscope is mainly determined by the size of the laser focus. Unfortunately, the diameter of the spot onto which the light can be focused is determined by the diffraction of the light at the limited aperture of the microscope's (objective) lens – approximately 200 nm for visible light (Abbe 1873; Hell 2007). However, addition of a second laser beam that switches off the fluorescence emission permits the observation of spots of nanoscopic size. Featuring a focal intensity distribution with at least one local intensity minimum (a zero-intensity point, e.g., at the focal center) this 'OFF' light beam selectively inhibits fluorescence everywhere but at the zero-intensity point. Scanning fluorescent images therefore constitute a huge improvement in spatial resolution. Reversible inhibition of fluorescence is realized by, for example, stimulated emission (STED), photoswitchable fluorophores (RESOLFT) or transient transitions to the fluorescent labels' metastable dark states (GSD).

In 2006, a new approach arose, referred to under a multitude of different acronyms such as STORM (Rust *et al.* 2006), (f)PALM (Betzig *et al.* 2006; Hess *et al.* 2006), Ground State Depletion Microscopy followed by individual molecule return (GSDIM) (Fölling *et al.* 2008), direct STORM (dSTORM) (Heilemann *et al.* 2008), or Single-Molecule Active Control Microscopy (SMACM) (Biteen *et al.* 2008). This approach relies on the stochastic on- and off-switching of the fluorescence emission of individual, well-separated labels combined with the determination of their exact spatial positions (Fig. 1b): usually, a large area of the sample is illuminated all at once and the spatial distribution of labeled molecules is determined by imaging the fluorescence onto a camera. Again, alike objects closer together than 200 nm cannot be distinguished, since because of the diffraction of light the image of a single point (PSF) appears blurred on the camera. By inhibiting the fluorescence emission of most of the labels, only single isolated molecules are allowed to fluoresce at a given time, and their spatial positions can be precisely determined from their blurred image spots on the camera using different localization approaches. By stochastically switching on and off different single isolated molecules in subsequent camera recordings, the final image with sub-diffraction sized spatial resolution is reconstructed from the summation of all localized spatial positions. It should be kept in mind that localization per se cannot provide sub-diffraction spatial resolution: separating alike objects at small distances requires a criterion to discern them from one another, such as switching them on and off in space and/or time (Hell and Wichmann 1994; Hell and Kroug 1995; Gordon *et al.* 2004; Qu *et al.* 2004; Lidke *et al.* 2005; Hell 2009b). This is why although it had been routinely applied for decades (see, e.g., Kusumi *et al.* 2005), specifically for spatio-temporal tracking of single isolated molecules, localization microscopy on its own did not provide images with sub-diffraction resolution.

The different nanoscopy techniques can record images with both multiple colors (e.g., Donnert *et al.* 2007; Bock *et al.* 2007; Bates *et al.* 2007; Schmidt *et al.* 2008; Huang *et al.* 2008; Juette *et al.* 2008; Shtengel *et al.* 2009; Pavani *et al.* 2009) and improved spatial resolution along all spatial directions (e.g., Klar *et al.* 2000; Harke *et al.* 2008; Schmidt *et al.* 2008). However, they each have their advantages and disadvantages with respect to for example photobleaching, set-up complexity, image acquisition speed and image reconstruction. For instance, a direct image of the spatial distribution of labeled molecules is formed in the scanning approach of the deterministic STED, GSD and RESOLFT nanoscopes, whereas a reconstruction algorithm based on the identification and localization of single isolated molecules needs to be employed to create the final image in the stochastic (d)STORM/(f)PALM/GSDIM

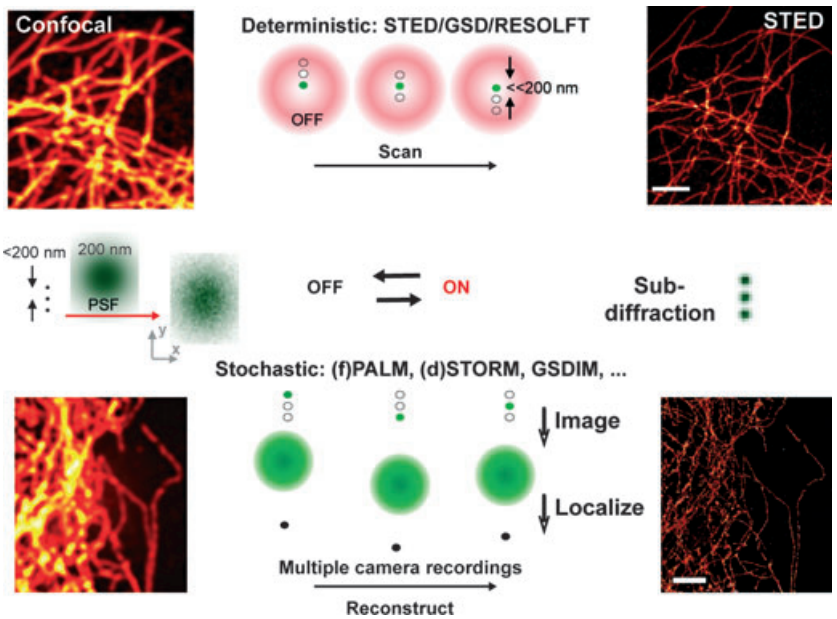

Fig. 1 Principle of far-field fluorescence nanoscopy. As a result of the diffraction of light, alike objects closer together than about 200 nm cannot be discerned when imaged with focused light [point-spread-function (PSF) ~ 200 nm in diameter], resulting in blurred images (left). Sub-diffraction images are realized by switching fluorescence on and off either in a deterministic or stochastic manner (middle), resulting in the ability to resolve structures < 200 nm in size (right). In the usual application of deterministic methods such as STED, GSD or RESOLFT, a diffraction-limited spot of the fluorescence excitation (ON) laser beam is overlaid with a second laser beam which switches off fluorescence emission and which features at least one zero-intensity point. Consequently, the off light selectively inhibits fluorescence everywhere but at the zero-intensity points, creating observation spots of nanoscopic size. Scanning fluorescence images therefore feature a considerable improvement in spatial resolution. Stochastic methods such as (f)PALM, (d)STORM, GSDIM are usually based on the recording of multiple wide-field images using a sensitive camera. During these recordings only single isolated molecules are allowed to fluoresce, and their position is determined using different localization approaches. By stochastically switching on and off all molecules during the recordings, the final image with sub-diffraction sized spatial resolution is reconstructed from the summation of all localized spatial positions.

approaches. Potential bias to the latter reconstruction process may arise for example from a lack of knowledge of missed or repeated recordings of molecules (Shroff *et al.* 2008; Small 2009). Furthermore, the determination of molecular positions may be biased for out-of-focus molecules (Enderlein *et al.* 2006; Engelhardt *et al.* 2011). Quite a number of improvements in the identification and localization algorithms have therefore been developed over the past years, especially aimed at image reconstructions for more densely labeled samples and/or those having low signal-to-noise levels (see, Dertinger *et al.* 2009; Cronin *et al.* 2009; Hedde *et al.* 2009; Smith *et al.* 2010; Larson 2010; Laurence and Chromy 2010; Henriques *et al.* 2010; Mortensen *et al.* 2010; Pertsinidis *et al.* 2010; Wolter *et al.* 2010; Endesfelder *et al.* 2010; Holden *et al.* 2011; Huang *et al.* 2011; Jones *et al.* 2011; Cox *et al.* 2012).

Photobleaching of the fluorescent labels is a more complex issue in deterministic-based nanoscopy: whereas in stochastic-based methods a molecule needs in principle to be switched on and off only once, the fluorescence has to be switched on and off multiple times during the scanning recording of the deterministic nanoscopy approaches, favoring labels and experimental conditions that supply this condition – we will come back to this issue later on. On the other hand, the image acquisition time of the stochastic (d)STORM/(f)PALM/GSDIM approaches is limited by the need to acquire sufficient molecular positions for the image reconstruction. Despite the aforementioned recent improvements in reconstruction algorithms there will potentially always be uncertainty as to whether the position of all molecules has been recorded, that is, of when to stop the acquisition, simply because these approaches are based on the stochastic on/off switching of fluorescence (see, e.g., Shroff *et al.* 2008; Small 2009). This is different for deterministic-based STED/GSD/RESOLFT approaches, where the scanning process defines the acquisition time. The use of fast beam scanners has established STED/RESOLFT nanoscopy as the currently fastest sub-diffraction imaging technique available, with up to 60–80 frames per second recording times for a few μm-sized observation areas (Westphal *et al.* 2008; Testa *et al.* 2012). In particular, the parallelization of the scanning procedure, that is, the

simultaneous scanning of multiple observation spots (such as realized for a structured illumination), leaves room for further improvement in the image acquisition speed of deterministic approaches (Heintzmann *et al.* 2002; Hell *et al.* 2003; Gustafsson 2005; Schwentker *et al.* 2007; Rego *et al.* 2012). The basic nanoscopy setups are usually expansions of conventional wide-field or (confocal) scanning microscopes by addition of an extra laser for switching fluorescence [note that confocality is not a requirement for the STED/GSD/RESOLFT concepts (Hell 2007)]. An initial concern of STED nanoscopy was the requirement for large, complex laser systems combined with the elaborate experimental procedure required to create zero-intensity point(s). However, recent advances in optical design and laser technology have permitted considerable simplification of the setups (Willig *et al.* 2007; Wildanger *et al.* 2008, 2009; Schrof *et al.* 2011; Vicidomini *et al.* 2011; Gould *et al.* 2012; Honigmann *et al.* 2012a; Mueller *et al.* 2012).

Most importantly, as they are based on the same principle of switching fluorescence on and off, the very same sample can be used for both targeted- and stochastic-based nanoscopy (Bretschneider 2007; Fölling *et al.* 2008; Brakemann *et al.* 2011). In view of the increased sensitivity and the aforementioned potential bias, both approaches can consequently be applied for the validation of results. Other approaches such as structured-illumination microscopy (SIM) (Gustafsson 2000; Schermelleh *et al.* 2008) or 4-Pi microscopy (Hell 1992; Gustafsson *et al.* 1995) are also often referred to as super-resolution microscopies. However, their spatial resolution is still limited (twofold improvement in spatial resolution for SIM and five to sixfold improvement in axial resolution for 4-Pi), that is they push the spatial resolution to the limits of the diffraction barrier. However, only the combination with reversible fluorescence inhibition processes can break these limits (Dyba and Hell 2002; Heintzmann *et al.* 2002; Hell *et al.* 2003; Gustafsson 2005; Schwentker *et al.* 2007; Rego *et al.* 2012). The fact that all the microscopy approaches are complementary, whether they are diffraction-limited or with nanoscale resolution, promotes research environments with access to various kinds of microscopes and nanoscopes, depending on their suitability for the case in hand.

STED nanoscopy: the road to live cell imaging

STED nanoscopy was not only the first nanoscopy technique to be developed, it was also the first to achieve cellular images with sub-diffraction spatial resolution (see, Klar *et al.* 2000; Willig *et al.* 2006b). Although a multitude of experiments over the past years have rendered STED imaging of fixed cells with down to 20 nm spatial resolution a generic tool for cellular studies, the potential phototoxic effect of the added STED light was long believed to be non-compatible with the study of living cells. Whereas the light intensities of the excitation laser are the same as in conventional confocal microscopy (1–10 μW), stimulated emission for example requires quite high light intensities of 1–10 MW/cm^2 at around 740–780 nm of the added STED laser (for example supplied by 100–300 mW average power of ~ 100–300 ps-long pulses of a titanium:sapphire laser), introducing the need to pay heed to heat absorption and light-induced toxic reactions. However, the involved peak intensities are smaller than those used in two-photon microscopy (Denk *et al.* 1990), a well-established tool in live-cell microscopy (Denk 1996). Further concerns about the addition of a STED laser arise from the increased photobleaching of the fluorescent label. This derives from the fact that the STED light acts on the excited fluorescent label. STED light *per se* is however not absorbed by the label and does not produce any photoreactive and thus -toxic species (unlike two-photon microscopy). Rather, stimulated emission shortens the time the fluorescent label spends in its excited (reactive) state and can reduce photoreactions such as photobleaching [compare with (Eggeling *et al.* 2005)]. Although excited state absorption of STED light can unfortunately cause severe photobleaching (Eggeling *et al.* 1998; Hotta *et al.* 2010), it was shown that fast scanning and the right choice of STED wavelength can minimize these effects (Donnert *et al.* 2009; Hotta *et al.* 2010; Moneron *et al.* 2010; Rankin *et al.* 2011). This is especially the case when using STED light in the range of 600 nm as required for live-cell labels such as green fluorescent protein (GFP) and its variants (Moneron *et al.* 2010; Rankin *et al.* 2011). Further, the use of a continuous-wave laser in conjunction with a gated fluorescence detection scheme has enabled a reduction in the STED laser power and a simplification of the setups (Vicidomini *et al.* 2011; Honigmann *et al.* 2012a; Mueller *et al.* 2012). As a consequence, STED microscopy is nowadays considered a straightforward technique for the study of the living cell using genetically encoded markers such as fluorescent proteins (Willig *et al.* 2006a; Hein *et al.* 2008; Nagerl *et al.* 2008; Eggeling *et al.* 2009; Li *et al.* 2009; Moneron and Hell 2009; Morozova *et al.* 2010; Rankin *et al.* 2011; Tonnesen *et al.* 2011; Urban *et al.* 2011), tagging proteins such as SNAP-, HALO-, or CLIP-tags (Schröder *et al.* 2008; Eggeling *et al.* 2009; Hein *et al.* 2010; Pellett *et al.* 2011; Lukinavicius *et al.* 2012), or fluorogen-activating tags (Fitzpatrick *et al.* 2009) (which both covalently bind functionalized and membrane-permeable organic dyes), even using commercial instrumentation (Schröder *et al.* 2008; Fitzpatrick *et al.* 2009; Morozova *et al.* 2010; Friedemann *et al.* 2011). Furthermore, the quite high laser intensities of 1–10 MW/cm^2 can be circumvented when switching from STED to RESOLFT nanoscopy, which employs laser intensities in the range of 1–5 kW/cm^2 only (Hofmann *et al.* 2005; Brakemann *et al.* 2011; Grotjohann *et al.* 2011; Testa *et al.* 2012). However, in contrast to STED, which can in principle employ any label, RESOLFT nanoscopy relies on

the use of special reversible photoswitchable molecules such as the reversible switchable GFP (rsGFP) (Grotjohann *et al.* 2011). Fortunately, the number of reversible switchable fluorescent proteins has significantly increased over the last years and their switching characteristics steadily improved (Grotjohann *et al.* 2012).

Live-cell STED microscopy in neuroscience

Confocal and two-photon microscopies have become common tools in Neurobiology, and have found wide application in the study of neuronal connections or processes, particularly those lying a few microns deep in, for example, cerebral cortex. It is important to study the neurons in living brain tissue and even the living animal, where all connections are preserved and functional. However, the diffraction-limited resolution of conventional far-field light microscopy is inadequate to resolve fine details, obliging researchers to complement the live-cell imaging with electron microscopy. This comes at a high cost, because the latter form of microscopy requires fixation, dehydration, embedding, thin cutting, and vacuum observation of the dehydrated nervous tissue. A case in point is the study of dendritic spines, the fine processes that form the post-synaptic compartment of central nervous system synapses. The majority of the excitatory synapses in the central nervous system are formed on dendritic spines. These micrometer/sub-micrometer-sized protrusions of the dendrite come in a variety of shapes: filopodia-like, stubby, cup-shaped, or mushroom shaped. Interestingly, dendritic spines show developmentally regulated and activity-dependent morphological changes. By adapting a STED microscope to the demands of *in vivo* imaging, the subtle dynamics of spines in the cerebral cortex of a living mouse were made visible (Fig. 2) (Berning *et al.* 2012). In living organotypic cultures of brain slices, it was shown that morphological parameters such as the neck width and curvature of the spine heads can be quantified to record changes, for example, induced by chemical long-term potentiation (cLTP) (Nagerl *et al.* 2008). The imaging of sub-cellular structures is also made possible with STED microscopy: actin, a key player in the morphological changes of synapses, can be visualized by STED microscopy. Using a fusion protein of Lifeact (a small peptide label for actin that does not disturb the actin polymerization or dynamics) and the yellow fluorescent protein (YFP), dynamic changes in actin molecules in synaptic spines located up to 120 μm deep in the cerebral tissue were observed (Urban *et al.* 2011). Establishment of either LTP or long-term depression (LTD) apparently requires a responsive F-actin cytoskeleton (Yuste and Bonhoeffer 2001). During neuronal development, a healthy cytoskeleton is essential for brain neurons to undergo the sequential steps of neurogenesis, cell migration and terminal differentiation (Ik-Tsen Heng *et al.* 2009). Nanoscopy studies of the actin cytoskeleton is gaining momentum in work on dendritic spines in brain (Tatavarty *et al.* 2011; Berning *et al.* 2012)·(Izeddin *et al.* 2011) and other cells and tissues (Xu *et al.* 2012). The localization of Na^+,K^+-ATPase has recently been accomplished using STED microscopy (Blom *et al.* 2011). Insight into the organization of protein complexes in the presynaptic active zone and post-synaptic density has also been gained with the aid of other nanoscopy techniques such as STORM (Dani *et al.* 2010). Endosomal

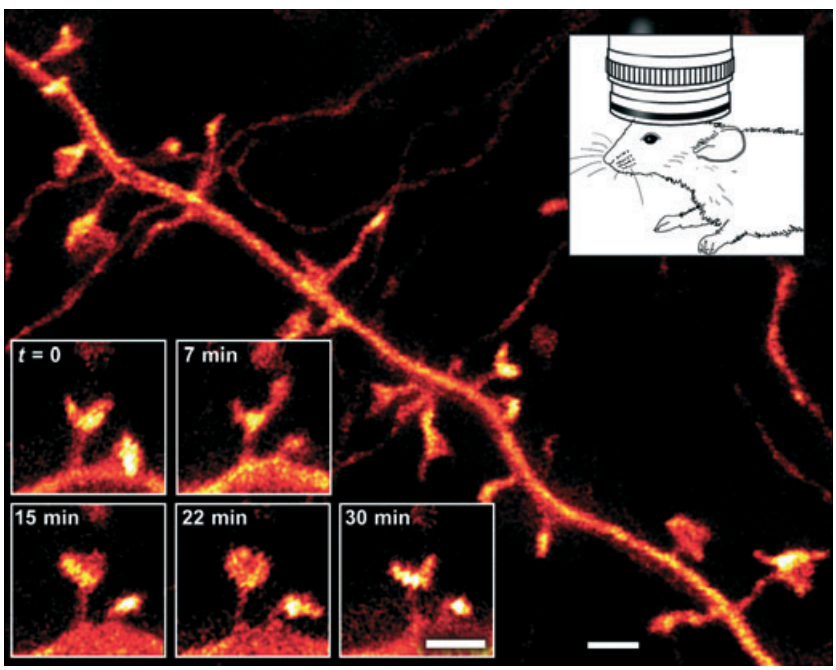

Fig. 2 Live-cell STED nanoscopy. STED imaging of the temporal dynamics of dendritic processes within the molecular layer of a TgN (Thy1-YFP) mouse, about 10–15 μm below the surface. Optical access to the visual cortex in the anesthetized mouse was provided by a glass sealed window. Scale bar: 1 μm. Adapted from (Berning *et al.* 2012).

sorting of vesicles in the presynapse has been analyzed in one of the few studies combining STED and electron microscopy (Hoopmann *et al.* 2010).

For imaging deep inside living tissue, STED microscopy has natural advantages over stochastic-based nanoscopy such as (d)STORM/(f)PALM/GSDIM. It provides sectioning capability and superior timing resolution. And, as shown by the various examples presented here, it can be a valuable tool in understanding basic working principles of the brain. Furthermore, it can be combined with two-photon excitation (Ding *et al.* 2009; Li *et al.* 2009; Moneron and Hell 2009; Bianchini and Diaspro 2012) or adaptive optics (Gould *et al.* 2012) for an optimized fluorescence excitation in deep tissue.

Live-cell STED microscopy of plasma membrane organization

A prominent example of the need for sub-diffraction resolution is the observation of plasma membrane heterogeneity such as in lipid–protein interactions, which are considered to play a functional part in a wide range of membrane-associated functionally relevant processes (see, e.g., Lingwood and Simons 2010). Unfortunately, many structural characteristics of the cellular membrane such as protein clusters, areas of different molecular order (often denoted lipid 'rafts'), or clathrin-coated pits are < 200 nm in size. Thus, their direct and non-invasive observation in the living cell is impeded by the resolution limit of > 200 nm of the conventional far-field fluorescence microscope. Over the last years, we have published several reports on the detection of nanoscopic membrane heterogeneities in the plasma membrane of living cells using the superior spatial resolution of STED nanoscopy. Besides directly imaging the organization of < 70 nm large protein clusters in the plasma membrane (Sieber *et al.* 2007), we could obtain new details of molecular membrane dynamics by combining a (tunable) resolution of down to 30 nm with tools such as fluorescence correlation spectroscopy (FCS) (Eggeling *et al.* 2009; Ringemann *et al.* 2009; Mueller *et al.* 2011; Honigmann *et al.* 2012b; Sezgin *et al.* 2012) (Fig. 3). In FCS, the transits

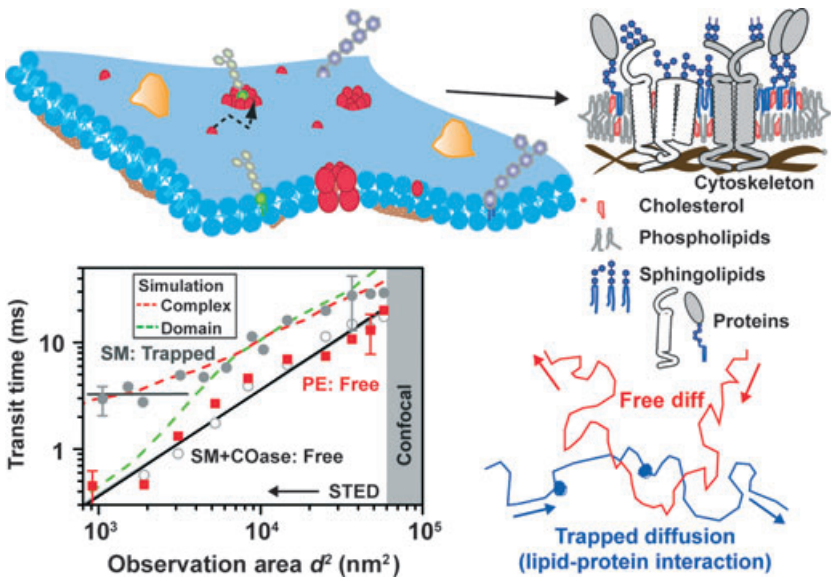

Fig. 3 Live-cell STED nanoscopy: STED-FCS analysis of lipid plasma membrane diffusion. (Upper panel) Lipids and proteins are heterogeneously distributed in the cellular plasma membrane, such distribution often stemming for example from cholesterol-assisted lipid–protein interactions (which may be the basis for the coalescence of transient signaling platforms – nanoscopic membrane domains termed lipid 'rafts', that is, spatially confined molecular assemblies of different lipids and proteins which are essential for certain transmembrane signaling events), or the underlying cytoskeleton (which is membrane-anchored via proteins). Adapted from (Lingwood and Simons 2010). (Lower left panel) The dependency of the transit time τ_D for different sub-diffraction sized observation areas $\sim d^2$ (as tuned by the STED laser power) shows an almost free diffusion (linear dependence, dark gray line diffusion coefficient 0.5 $\mu m^2/s$) for a fluorescent phospholipid analogue (phosphoethanolamine, PE, red squares), and a hindered diffusion (non-linear dependence) for a fluorescent sphingolipid analogue (sphingomyelin, SM, gray circles). Depletion of cholesterol by cholesterol oxidase (COase) reduces hindrances in molecular diffusion of SM (SM+COase, open circles). The minimal change in τ_D for very small observation areas (gray horizontal line) and Monte-Carlo simulations indicate that the hindrance in diffusion is caused by transient complexes with either relatively slow-moving or immobilized membrane molecules (red dotted line) and not by incorporation into $\geq$ 20 nm large domains, where diffusion is slowed down (green dotted line). Direct observation of these transient interactions is impossible with the large diffraction-limited confocal observation area (gray shaded area). (Lower right panel) Schematic drawing of normal free (red) and hindered SM diffusion (blue, dots: points of interactions or complexes).

of single molecules through a usually fixed observation spot are observed to determine dynamic parameters such as the average transit time (Magde *et al.* 1972; Ehrenberg and Rigler 1974; Haustein and Schwille 2003). Investigating the dependence of the average transit time on the size of the observation spot highlights hindrances in molecular diffusion such as transient molecular interactions (Wawrezinieck *et al.* 2005). STED nanoscopy is a perfect tool for these studies as it allows a straightforward variation of the observation spot size by, for example, variation of the power of the STED laser (Eggeling 2012). Our STED-FCS experiments revealed that sphingolipids and certain proteins are transiently (~ 10 ms) trapped on the nanoscale in often cholesterol-mediated and/or cytoskeleton-associated molecular complexes, whereas other molecules diffuse freely (Mueller *et al.* 2011). Different lipid structures show up distinctly, but so far at least such differences do not appear to be because of variations in the labeling. We observed strong differences in the molecular nature behind the nanoscopic molecular interactions as observed by STED-FCS and the separation of membranes into liquid-disordered and -ordered phases (Mueller *et al.* 2011; Sezgin *et al.* 2012). Specifically the latter phase is often referred to as being an appropriate physical model of lipid nanodomains, the so-called lipid 'rafts'. Together with a suitable fluorescent lipid marker for the liquid-ordered phase, STED-FCS has the potential to shed new light on the mystery and functionality of these lipid nanodomains (Honigmann *et al.* 2012b).

STED-FCS is very similar to single-molecule or -particle tracking (SPT), which is also often applied to investigate diffusion characteristics of membrane components (e.g., Kusumi *et al.* 2005; Wieser *et al.* 2007; Manley *et al.* 2008; Sahl *et al.* 2010). While SPT allows the direct visualization of the diffusion path of individual molecules and thus of any (even less abundant) hindrances, it requires much longer recording times and more detailed data analysis than FCS to obtain average molecular characteristics of high statistical accuracy. Nevertheless, both STED-FCS and SPT, and more so their complementary applications, have the potential to revolutionize our understanding of membrane bioactivity (e.g., Kusumi *et al.* 2010; Eggeling 2012).

Conclusions

It is highly likely that the novel possibilities of far-field fluorescence STED nanoscopy described in this short review will contribute to our understanding of the living cell in general, and will shed new light on a whole range of cellular phenomena, including key neurobiological processes such as development, pruning, and stabilization of synapses, their subtle dynamic changes triggered by chemical or electrical stimulation, and the possible alteration of these processes in disease. Likewise, the new nanoscopies are ideally suited to address important issues in membrane biology which are bound to find answers at the nanoscale, such as lipid–protein interactions and nanodomains in membrane bioactivity and receptor signaling in neurobiology and cell biology at large.

Conflicts of interest

The authors declare no conflicts of interest.

References

Abbe E. (1873) Beiträge zur Theorie des Mikroskops und der mikroskopischen Wahrnehmung. *Archiv für Mikroskopische Anatomie* **9**, 413–468.

Bates M., Huang B., Dempsey G. T. and Zhuang X. W. (2007) Multicolor super-resolution imaging with photo-switchable fluorescent probes. *Science* **317**, 1749–1753.

Bates M., Huang B. and Zhuang X. W. (2008) Super-resolution microscopy by nanoscale localization of photo-switchable fluorescent probes. *Curr. Opin. Chem. Biol.* **12**, 505–514.

Berning S., Willig K. I., Steffens H., Dibaj P. and Hell S. W. (2012) Nanoscopy in a living mouse brain. *Science* **335**, 551.

Betzig E., Patterson G. H., Sougrat R., Lindwasser O. W., Olenych S., Bonifacino J. S., Davidson M. W., Lippincott-Schwartz J. and Hess H. F. (2006) Imaging intracellular fluorescent proteins at nanometer resolution. *Science* **313**, 1642–1645.

Bianchini P. and Diaspro A. (2012) Fast scanning STED and two-photon fluorescence excitation microscopy with continuous wave beam. *J. Microsc.* **245**, 225–228.

Biteen J. S., Thompson M. A., Tselentis N. K., Bowman G. R., Shapiro L. and Moerner W. E. (2008) Super-resolution imaging in live caulobacter crescentus cells using photoswitchable EYFP. *Nat. Methods* **5**, 947–949.

Blom H., Rönnlund D., Scott L., Spicarova Z., Widengren J., Bondar A., Aperia A. and Brismar H. (2011) Spatial distribution of Na+-K + -ATPase in dendritic spines dissected by nanoscale superresolution STED microscopy. *BMC Neurosci.* **12**, 16.

Bock H., Geisler C., Wurm C. A., Von Middendorff C., Jakobs S., Schonle A., Egner A., Hell S. W. and Eggeling C. (2007) Two-color far-field fluorescence nanoscopy based on photoswitchable emitters. *Appl. Phys. B* **88**, 161–165.

Brakemann T., Stiel A. C., Weber G. *et al.* (2011) A reversibly photoswitchable GFP-like protein with fluorescence excitation decoupled from switching. *Nat. Biotechnol.* **29**, 942–947.

Bretschneider S. (2007) *Ground-State-Depletion Fluorescence Microscopy*. University Goettingen, Goettingen.

Bretschneider S., Eggeling C. and Hell S. W. (2007) Breaking the diffraction barrier in fluorescence microscopy by optical shelving. *Phys. Rev. Lett.* **98**, 218103.

Chi K. R. (2009) Super-resolution microscopy: breaking the limits. *Nat. Methods* **6**, 15–18.

Cox S., Rosten E., Monypenny J., Jovanovic-Talisman T., Burnette D. T., Lippincott-Schwartz J., Jones G. E. and Heintzmann R. (2012) Bayesian localization microscopy reveals nanoscale podosome dynamics. *Nat. Methods* **9**, 195–200.

Cronin B., de Wet B. and Wallace M. I. (2009) Lucky imaging: improved localization accuracy for single molecule imaging. *Biophys. J.* **96**, 2912–2917.

Dani S., Huang B., Bergan J., Dulac C. and Zhuang X. (2010) Superresolution imaging of chemical synapses in the brain. *Neuron* **68**, 843–856.

Dedecker P., Hofkens J. and Hotta J. I. (2008) Diffraction-unlimited optical microscopy. *Mater. Today* **11**, 12–21.

Dempsey G. T., Vaughan J. C., Chen K. H., Bates M. and Zhuang X. (2011) Evaluation of fluorophores for optimal performance in localization-based super-resolution imaging. *Nat. Methods* **8**, 1027–1036.

Denk W. (1996) Two-photon excitation in functional biological imaging. *J. Biomed. Opt.* **1**, 296–304.

Denk W., Strickler J. H. and Webb W. W. (1990) 2-photon laser scanning fluorescence microscopy. *Science* **248**, 73–76.

Dertinger T., Colyer R., Iyer G., Weiss S. and Enderlein J. (2009) Fast, background-free, 3D super-resolution optical fluctuation imaging (SOFI). *PNAS* **106**, 22287–22292.

Ding J. B., Takasaki K. T. and Sabatini B. L. (2009) Supraresolution imaging in brain slices using stimulated-emission depletion two-photon laser scanning microscopy. *Neuron* **63**, 429–437.

Donnert G., Keller J., Wurm C. A. *et al.* (2007) Two-color far-field fluorescence nanoscopy. *Biophys. J.* **92**, L67–L69.

Donnert G., Eggeling C. and Hell S. W. (2009) Triplet-relaxation microscopy with bunched pulsed excitation. *Photochem. Photobiol.* **8**, 481–485.

Dyba M. and Hell S. W. (2002) Focal spots of size lambda/23 open up far-field florescence microscopy at 33 nm axial resolution. *Phys. Rev. Lett.* **88**, 163901.

Eggeling C. (2012) STED-FCS nanoscopy of membrane dynamics, in *Fluorescent Methods to Study Biological Membranes* (Mely Y. and Duportail G., eds), pp. 291–309. Springer-Verlag, Berlin.

Eggeling C., Widengren J., Rigler R. and Seidel C. A. M. (1998) Photobleaching of fluorescent dyes under conditions used for single-molecule detection: Evidence of two-step photolysis. *Anal. Chem.* **70**, 2651–2659.

Eggeling C., Volkmer A. and Seidel C. A. M. (2005) Molecular photobleaching kinetics of Rhodamine 6G by one- and two-photon induced confocal fluorescence microscopy. *ChemPhysChem* **6**, 791–804.

Eggeling C., Ringemann C., Medda R. *et al.* (2009) Direct observation of the nanoscale dynamics of membrane lipids in a living cell. *Nature* **457**, 1159–U1121.

Ehrenberg M. and Rigler R. (1974) Rotational brownian motion and fluorescence intensity fluctuations. *Chem. Phys.* **4**, 390–401.

Enderlein J., Toprak E. and Selvin P. R. (2006) Polarization effect on position accuracy of fluorophore localization. *Opt. Express* **14**, 8111–8120.

Endesfelder U., van de Linde S., Wolter S., Sauer M. and Heilemann M. (2010) Subdiffraction-resolution fluorescence microscopy of myosin–actin motility. *ChemPhysChem* **11**, 836–840.

Engelhardt J., Keller J., Hoyer P., Reuss M., Staudt T. and Hell S. W. (2011) Molecular orientation affects localization accuracy in superresolution far-field fluorescence microscopy. *Nano Lett.* **11**, 8066–8072.

Evanko D. (2009) Primer: fluorescence imaging under the diffraction limit. *Nat. Methods* **6**, 19–20.

Fernandez-Suarez M. and Ting A. Y. (2008) Fluorescent probes for super-resolution imaging in living cells. *Nat. Rev. Mol. Cell Biol.* **9**, 929–943.

Fitzpatrick J. A., Yan Q., Sieber J. J. *et al.* (2009) STED nanoscopy in living cells using fluorogen activating proteins. *Bioconjug. Chem.* **20**, 1843–1847.

Fölling J., Bossi M., Bock H., Medda R., Wurm C. A., Hein B., Jakobs S., Eggeling C. and Hell S. W. (2008) Fluorescence nanoscopy by ground-state depletion and single-molecule return. *Nat. Methods* **5**, 943–945.

Friedemann K., Turshatov A., Landfester K. and Crespy D. (2011) Characterization via two-color STED microscopy of nanostructured materials synthesized by colloid electrospinning. *Langmuir* **27**, 7132–7139.

Gordon M. P., Ha T. and Selvin P. R. (2004) Single-molecule high-resolution imaging with photobleaching. *PNAS* **101**, 6462–6465.

Gould T. J., Burke D., Bewersdorf J. and Booth M. J. (2012) Adaptive optics enables 3D STED microscopy in aberrating specimens. *Opt. Express* **20**, 20998.

Grotjohann T., Testa I., Leutenegger M. *et al.* (2011) Diffraction-unlimited all-optical imaging and writing with a photochromic GFP. *Nature* **478**, 204–208.

Grotjohann T., Testa I., Reuss M., Brakemann T., Eggeling C., Hell S. W. and Jakobs S. (2012) rsEGFP2 enables fast RESOLFT nanoscopy of living cells. *Elife* **1**, e00248.

Gustafsson M. G. L. (2000) Surpassing the lateral resolution limit by a factor of two using structured illumination microscopy. *J. Microsc.* **198**, 82–87.

Gustafsson M. G. L. (2005) Nonlinear structured-illumination microscopy: Wide-field fluorescence imaging with theoretically unlimited resolution. *PNAS* **102**, 13081–13086.

Gustafsson M. G. L., Agard D. A. and Sedat J. W. (1995) Sevenfold improvement of axial resolution in 3D widefield microscopy using two objective lenses. *Proc. Soc. Photo Opt. Instrum. Eng.* **2412**, 147–156.

Han K. Y., Kim S. K., Eggeling C. and Hell S. (2010) Metastable dark states enable ground state depletion microscopy of nitrogen vacancy centers in diamond with diffraction-unlimited resolution. *Nano Lett.* **10**, 3199–3203.

Harke B., Ullal C. K., Keller J. and Hell S. W. (2008) Three-dimensional nanoscopy of colloidal crystals. *Nano Lett.* **8**, 1309–1313.

Haustein E. and Schwille P. (2003) Ultrasensitive investigations of biological systems by fluorescence correlation spectroscopy. *Methods* **29**, 153–166.

Hedde P. N., Fuchs J., Oswald F., Wiedenmann J. and Nienhaus G. U. (2009) Online image analysis software for photoactivation localization microscopy. *Nat. Methods* **6**, 689–690.

Heilemann M., van de Linde S., Schuttpelz M., Kasper R., Seefeldt B., Mukherjee A., Tinnefeld P. and Sauer M. (2008) Subdiffraction-resolution fluorescence imaging with conventional fluorescent probes. *Angew. Chem. Int. Ed. Engl.* **47**, 6172–6176.

Heilemann M., Dedecker P., Hofkens J. and Sauer M. (2009) Photoswitches: key molecules for subdiffraction-resolution fluorescence imaging and molecular quantification. *Laser Photon. Rev.* **3**, 180–202.

Hein B., Willig K. I. and Hell S. W. (2008) Stimulated emission depletion (sted) nanoscopy of a fluorescent protein-labeled organelle inside a living cell. *PNAS* **105**, 14271–14276.

Hein B., Willig K. I., Wurm C. A., Westphal V., Jakobs S. and Hell S. W. (2010) Stimulated emission depletion nanoscopy of living cells using snap-tag fusion proteins. *Biophys. J.* **98**, 158–163.

Heintzmann R. and Ficz G. (2007) Breaking the resolution limit in light microscopy. *Methods Cell Biol.* **81**, 561–580.

Heintzmann R. and Gustafsson M. G. L. (2009) Subdiffraction resolution in continuous samples. *Nat. Photonics* **3**, 362–364.

Heintzmann R., Jovin T. M. and Cremer C. (2002) Saturated patterned excitation microscopy - A concept for optical resolution improvement. *J. Opt. Soc. Am. A Opt. Image Sci. Vis.* **19**, 1599–1609.

Hell S. W. (1992) *Double-scanning confocal microscope*. European Patent, Vol. 0491289.

Hell S. W. (2003) Toward fluorescence nanoscopy. *Nat. Biotechnol.* **21**, 1347–1355.

Hell S. W. (2004) Strategy for far-field optical imaging and writing without diffraction limit. *Phys. Lett. A* **326**, 140–145.

Hell S. W. (2007) Far-field optical nanoscopy. *Science* **316**, 1153–1158.

Hell S. (2009a) Far-field optical nanoscopy, in *Single Molecule Spectroscopy in Chemistry* (Gräslund A., Rigler R. and Widengren J., eds), pp. 365–398. Springer, Berlin.

Hell S. W. (2009b) Microscopy and its focal switch. *Nat. Methods* **6**, 24–32.

Hell S. W. and Kroug M. (1995) Ground-state depletion fluorescence microscopy, a concept for breaking the diffraction resolution limit. *Appl. Phys. B* **60**, 495–497.

Hell S. W. and Wichmann J. (1994) Breaking the diffraction resolution limit by stimulated-emission - stimulated-emission-depletion fluorescence microscopy. *Opt. Lett.* **19**, 780–782.

Hell S. W., Jakobs S. and Kastrup L. (2003) Imaging and writing at the nanoscale with focused visible light through saturable optical transitions. *Appl. Phys. A* **77**, 859–860.

Hell S. W., Dyba M. and Jakobs S. (2004) Concepts for nanoscale resolution in fluorescence microscopy. *Curr. Opin. Neurobiol.* **14**, 599–609.

Henriques R., Lelek M., Fornasiero E. F., Valtorta F., Zimmer C. and Mhlanga M. M. (2010) QuickPALM: 3D real-time photoactivation nanoscopy image processing in ImageJ. *Nat. Methods* **7**, 339–340.

Hess S. T., Girirajan T. P. K. and Mason M. D. (2006) Ultra-high resolution imaging by fluorescence photoactivation localization microscopy. *Biophys. J.* **91**, 4258–4272.

Hofmann M., Eggeling C., Jakobs S. and Hell S. W. (2005) Breaking the diffraction barrier in fluorescence microscopy at low light intensities by using reversibly photoswitchable proteins. *PNAS* **102**, 17565–17569.

Holden S. J., Uphoff S. and Kapanidis A. N. (2011) DAOSTORM: an algorithm for highdensity super-resolution microscopy. *Nat. Methods* **8**, 279–280.

Honigmann A., Eggeling C., Schulze M. and Lepert A. (2012a) Super-resolution STED microscopy advances with yellow CW OPSL. *Laser Focus World* **48**, 75–79.

Honigmann A., Mueller V., Hell S. W. and Eggeling C. (2012b) STED microscopy detects and quantifies liquid phase separation in lipid membranes using a new far-red emitting fluorescent phosphoglycerolipid analogue. *Faraday Discussions* **161**, 77–89. doi:10.1039/C2FD20107K.

Hoopmann P., Punge A., Baryscha S. V. *et al.* (2010) Endosomal sorting of readily releasable synaptic vesicles. *PNAS* **107**, 19055–19060.

Hotta J., Fron E., Dedecker P. *et al.* (2010) Spectroscopic Rationale for efficient stimulated-emission depletion microscopy fluorophores. *J. Am. Chem. Soc.* **132**, 5021–5023.

Huang B. (2010) Super-resolution optical microscopy: multiple choices. *Curr. Opin. Chem. Biol.* **14**, 10–14.

Huang B., Wang W. Q., Bates M. and Zhuang X. W. (2008) Three-dimensional super-resolution imaging by stochastic optical reconstruction microscopy. *Science* **319**, 810–813.

Huang B., Bates M. and Zhuang X. (2009) Super-resolution fluorescence microscopy. *Annu. Rev. Biochem.* **78**, 993–1016.

Huang B., Babcock H. and Zhuang X. (2010) Breaking the diffraction barrier: super-resolution imaging of cells. *Cell* **143**, 1047–1058.

Huang F., Schwartz S. L., Byars J. M. and Lidke K. A. (2011) Simultaneous multiple-emitter fitting for single molecule super-resolution imaging. *Biomed. Opt. Express* **2**, 1377–1393.

Ik-Tsen Heng J., Chariot A. and Nguyen L. (2009) Molecular layers underlying cytoskeletal remodelling during cortical development. *Trends Neurosci.* **33**, 38–46.

Izeddin I., Specht C. G., Lelek M., Darzacq X., Triller A., Zimmer C. and Dahan M. (2011) Super-resolution dynamic imaging of dendritic spines using a low-affinity photoconvertible actin probe. *PLoS ONE* **6**, e15611.

Jones S. A., Shim S.-H., He J. and Zhuang X. (2011) Fast, three-dimensional super-resolution imaging of live cells. *Nat. Methods* **8**, 499–505.

Juette M. F., Gould T. J., Lessard M. D., Mlodzianoski M. J., Nagpure B. S., Bennett B. T., Hess S. T. and Bewersdorf J. (2008) Three-dimensional sub-100 nm resolution fluorescence microscopy of thick samples. *Nat. Methods* **5**, 527–529.

Klar T. A., Jakobs S., Dyba M., Egner A. and Hell S. W. (2000) Fluorescence microscopy with diffraction resolution barrier broken by stimulated emission. *PNAS* **97**, 8206–8210.

Kusumi A., Nakada C., Ritchie K., Murase K., Suzuki K., Murakoshi H., Kasai R. S., Kondo J. and Fujiwara T. (2005) Paradigm shift of the plasmamembrane concept from the two-dimensional continuum fluid to the partitioned fluid: High-speed single-molecule tracking of membrane molecules. *Annu. Rev. Biophys.* **34**, 351–378.

Kusumi A., Shirai Y. M., Koyama-Honda I., Suzuki K. G. N. and Fujiwara T. K. (2010) Hierarchical organization of the plasma membrane: investigations by single-molecule tracking vs. fluorescence correlation spectroscopy. *FEBS Lett.* **584**, 1814–1823.

Larson D. R. (2010) The economy of photons. *Nat. Methods* **7**, 357–359.

Laurence T. A. and Chromy B. A. (2010) Efficient maximum likelihood estimator fitting of histograms. *Nat. Methods* **5**, 338–339.

Li Q., Wu S. S. H. and Chou K. C. (2009) Subdiffraction-limit two-photon fluorescence microscopy for GFP-tagged cell imaging. *Biophys. J.* **97**, 3224–3228.

Lidke K. A., Rieger B., Jovin T. M. and Heintzmann R. (2005) Superresolution by localization of quantum dots using blinking statistics. *Opt. Express* **13**, 7052–7062.

Lingwood D. and Simons K. (2010) Lipid rafts as a membrane-organizing principle. *Science* **327**, 46–50.

Lippincott-Schwartz J. and Manley S. (2009) Putting super-resolution fluorescence microscopy to work. *Nat. Methods* **6**, 21–23.

Lukinavicius G., Umezawa K., Olivier N. *et al.* (2012) A near-infrared fluorophore for live-cell superresolution microscopy of cellular proteins. *Nat. Chem.* **5**, 132–139. doi:10.1038/NCHEM.1546.

Magde D., Webb W. W. and Elson E. (1972) Thermodynamic fluctuations in a reacting system - measurement by fluorescence correlation spectroscopy. *Phys. Rev. Lett.* **29**, 705–708.

Manley S., Gillette J. M., Patterson G. H., Shroff H., Hess H. F., Betzig E. and Lippincott-Schwartz J. (2008) High-density mapping of single-molecule trajectories with photoactivated localization microscopy. *Nat. Methods* **5**, 155–157.

Moerner W. E. (2006) Single-molecule mountains yield nanoscale cell images. *Nat. Methods* **3**, 781–782.

Moneron G. and Hell S. (2009) Two-photon excitation STED microscopy. *Opt. Express* **17**, 14567–14573.

Moneron G., Medda R., Hein B., Giske A., Westphal V. and Hell S. W. (2010) Fast STED microscopy with continuous wave fiber lasers. *Opt. Express* **18**, 1302–1309.

Morozova K. S., Piatkevich K. D., Gould T. J., Zhang J., Bewersdorf J. and Verkhusha V. V. (2010) Far-red fluorescent protein excitable with red lasers for flow cytometry and superresolution STED nanoscopy. *Biophys. J.* **99**, L13–L15.

Mortensen K. I., Churchman S. L., Spudich J. A. and Flyvbjerg H. (2010) Optimized localization analysis for single-molecule tracking and super-resolution microscopy. *Nat. Methods* **7**, 377–381.

Mueller V., Ringemann C., Honigmann A. *et al.* (2011) STED nanoscopy reveals molecular details of cholesterol- and cytoskeleton-modulated lipid interactions in living cells. *Biophys. J.* **101**, 1651–1660.

Mueller V., Eggeling C., Karlsson H. and von Gegerfelt D. (2012) CW DPSS lasers make STED microscopy more practical. *Biophotonics* **19**, 30–32.

Muller T., Schumann C. and Kraegeloh A. (2012) STED Microscopy and its applications: new insights into cellular processes on the nanoscale. *ChemPhysChem* **13**, 1986–2000.

Nagerl U. V., Willig K. I., Hein B., Hell S. W. and Bonhoeffer T. (2008) Live-cell imaging of dendritic spines by STED microscopy. *PNAS* **105**, 18982–18987.

Patterson G., Davidson M., Manley S. and Lippincott-Schwartz J. (2010) Superresolution imaging using single-molecule localization. *Annu. Rev. Phys. Chem.* **61**, 345–367.

Pavani S. R. P., Thompson M. A., Biteen J. S., Lord S. J., Liu N., Twieg R. J., Piestun R. and Moerner W. E. (2009) Three-dimensional, single-molecule fluorescence imaging beyond the diffraction limit by using a double-helix point spread function. *PNAS* **106**, 2995–2999.

Pellett P. A., Sun X., Gould T. J., Rothman J. E., Xu M.-Q., Correa I. R. Jr and Bewersdorf J. (2011) Two-color STED microscopy in living cells. *Biomed. Opt. Express* **2**, 2364–2371.

Pertsinidis A., Zhang Y. and Chu S. (2010) Subnanometre single-molecule localization, registration and distance measurements. *Nature* **466**, 647–651.

Qu X. H., Wu D., Mets L. and Scherer N. F. (2004) Nanometer-localized multiple single-molecule fluorescence microscopy. *PNAS* **101**, 11298–11303.

Rankin B. R., Moneron G., Wurm C. A., Nelson J. C., Walter A., Schwarzer D., Schroeder J., Colon-Ramos D. A. and Hell S. W. (2011) Nanoscopy in a living multicellular organism expressing GFP. *Biophys. J.* **100**, L63–L65.

Rego E. H., Shao L., Macklin J. J., Winoto L., Johansson G. A., Kamps-Hughes N., Davidson M. W. and Gustafsson M. G. L. (2012) Nonlinear structured-illumination microscopy with a photoswitchable protein reveals cellular structures at 50-nm resolution. *PNAS* **109**, E135–E143.

Rice J. H. (2007) Beyond the diffraction limit: far-field fluorescence imaging with ultrahigh resolution. *Mol. BioSyst.* **3**, 781–793.

Ringemann C., Harke B., Middendorff C. V. *et al.* (2009) Exploring single-molecule dynamics with fluorescence nanoscopy. *New J. Phys.* **11**, 103054.

Rust M. J., Bates M. and Zhuang X. W. (2006) Sub-diffraction-limit imaging by stochastic optical reconstruction microscopy (STORM). *Nat. Methods* **3**, 793–795.

Sahl S. J., Leutenegger M., Hilbert M., Hell S. W. and Eggeling C. (2010) Fast molecular tracking maps nanoscale dynamics of plasma membrane lipids. *PNAS* **107**, 6829–6834.

Schermelleh L., Carlton P. M., Haase S. *et al.* (2008) Subdiffraction multicolor imaging of the nuclear periphery with 3D structured illumination microscopy. *Science* **320**, 1332–1336.

Schmidt R., Wurm C. A., Jakobs S., Engelhardt J., Egner A. and Hell S. W. (2008) Spherical nanosized focal spot unravels the interior of cells. *Nat. Methods* **5**, 539–544.

Schröder J., Benink H., Dyba M. and Los G. V. (2008) *In vivo* labeling method using a genetic construct for nanoscale resolution microscopy. *Biophys. J.* **96**, L1–L3.

Schrof S., Staudt T., Rittweger E., Wittenmayer N., Dresbach T., Engelhardt J. and Hell S. W. (2011) STED nanoscopy with mass-produced laser diodes. *Opt. Express* **19**, 8066–8072.

Schwentker M. A., Bock H., Hofmann M., Jakobs S., Bewersdorf J., Eggeling C. and Hell S. W. (2007) Wide-field subdiffraction RESOLFT microscopy using fluorescent protein photoswitching. *Microsc. Res. Tech.* **70**, 269–280.

Sezgin E., Levental I., Grzybek M. *et al.* (2012) Partitioning, diffusion, and ligand binding of raft lipid analogs in model and cellular plasma membranes.. *Biochimica et Biophysica Acta (BBA) - Biomembranes* **1818**, 1777–1784.

Shroff H., Galbraith C. G., Galbraith J. A. and Betzig E. (2008) Live-cell photoactivated localization microscopy of nanoscale adhesion dynamics. *Nat. Methods* **5**, 417–423.

Shtengel G., Galbraith J. A., Galbraith C. G. *et al.* (2009) Interferometric fluorescent super-resolution microscopy resolves 3D cellular ultrastructure. *PNAS* **106**, 3125–3130.

Sieber J. J., Willig K. I., Kutzner C. *et al.* (2007) Anatomy and dynamics of a supramolecular membrane protein cluster. *Science* **317**, 1072–1076.

Small A. R. (2009) Theoretical limits on errors and acquisition rates in localizing switchable fluorophores. *Biophys. J.* **96**, L16–L18.

Smith C. S., Joseph N., Rieger B. and Lidke K. A. (2010) Fast, single-molecule localization that achieves theoretically minimum uncertainty. *Nat. Methods* **7**, 373–375.

Tatavarty V., Eun-Ji Kim E.-J., Rodionov V. and Yu J. (2011) Investigating sub-spine actin dynamics in rat hippocampal neurons with super-resolution optical imaging. *PLoS ONE* **4**, e7724.

Testa I., Urban N. T., Jakobs S., Eggeling C., Willig K. I. and Hell S. W. (2012) Nanoscopy of living brain slices with low light levels. *Neuron* **75**, 992–1000.

Tonnesen J., Nadrigny F., Willig K. I., Wedlich-Soldner R. and Nagerl U. V. (2011) Two-color STED microscopy of living synapses using a single laser-beam pair. *Biophys. J.* **101**, 2545–2552.

Urban N. T., Willig K. I., Hell S. W. and Nagerl U. V. (2011) STED Nanoscopy of actin dynamics in synapses deep inside living brain slices. *Biophys. J.* **101**, 1277–1284.

Vicidomini G., Moneron G., Han K. Y., Westphal V., Ta H., Reuss M., Engelhardt H., Eggeling C. and Hell S. W. (2011) Sharper low-power STED nanoscopy by time gating. *Nat. Methods* **8**, 571–573.

Wawrezinieck L., Rigneault H., Marguet D. and Lenne P. F. (2005) Fluorescence correlation spectroscopy diffusion laws to probe the submicron cell membrane organization. *Biophys. J.* **89**, 4029–4042.

Westphal V., Rizzoli S. O., Lauterbach M. A., Kamin D., Jahn R. and Hell S. W. (2008) Video-rate far-field optical nanoscopy dissects synaptic vesicle movement. *Science* **320**, 246–249.

Wieser S., Moertelmaier M., Fuertbauer E., Stockinger H. and Schutz G. (2007) (Un)Confined diffusion of CD59 in the plasma membrane determined by high-resolution single molecule microscopy. *Biophys. J.* **92**, 3719–3728.

Wildanger D., Rittweger E., Kastrup L. and Hell S. W. (2008) STED microscopy with a supercontinuum laser source. *Opt. Express* **16**, 9614–9621.

Wildanger D., Bückers J., Westphal V., Hell S. W. and Kastrup L. (2009) A STED microscope aligned by design. *Opt. Express* **17**, 16100–16110.

Willig K. I., Kellner R. R., Medda R., Hein B., Jakobs S. and Hell S. W. (2006a) Nanoscale resolution in GFP-based microscopy. *Nat. Methods* **3**, 721–723.

Willig K. I., Rizzoli S. O., Westphal V., Jahn R. and Hell S. W. (2006b) Sted microscopy reveals that synaptotagmin remains clustered after synaptic vesicle exocytosis. *Nature* **440**, 935–939.

Willig K. I., Harke B., Medda R. and Hell S. W. (2007) STED microscopy with continuous wave beams. *Nat. Methods* **4**, 915–918.

Wolter S., Schuttpelz M., Tscherepanow M., van de Linde S., Heilemann M. and Sauer M. (2010) Real-time computation of subdiffraction-resolution fluorescence images. *J. Microsc.* **237**, 12–22.

Xu K., Babcock H. P. and Zhuang X. (2012) Dual-objective STORM reveals three-dimensional filament organization in the actin cytoskeleton. *Nat. Methods* **9**, 185–188.

Yuste R. and Bonhoeffer T. (2001) Morphological changes in dendritic spines associated with long-term synaptic plasticity. *Annu. Rev. Neurosci.* **24**, 1071–1089.